Tumor Biol. (2016) 37:1173–1182
DOI 10.1007/s13277-015-3790-7

ORIGINAL ARTICLE

Expression profiling of angiogenesis-related genes in brain metastases of lung cancer and melanoma

Aysegül Ilhan-Mutlu[1,6] · Christian Siehs[2] · Anna Sophie Berghoff[1,6] · Gerda Ricken[3] · Georg Widhalm[4,6] · Ludwig Wagner[5,6] · Matthias Preusser[1,6,7]

Received: 18 May 2015 / Accepted: 9 July 2015 / Published online: 16 August 2015

Abstract Brain metastases (BM) are the most common brain tumors of adults and are associated with fatal prognosis. Formation of new blood vessels, named angiogenesis, was proposed to be the main hallmark of the growth of BM. Previous preclinical evidence revealed that angiogenic blockage might be considered for treatment; however, there were varying responses. In this study, we aimed to characterize the expression pattern of angiogenesis-related genes in BM of lung cancer and melanoma, which might be of importance for the different responses against anti-angiogenic treatment. Fifteen snap-frozen tissues obtained from BM of non-small cell lung cancer (NSCLC), small-cell lung cancer (SCLC), and melanoma patients were analyzed for angiogenesis-related genes using a commercially available gene expression kit. Epilepsy tissue was used as control. Expression values were analyzed using hierarchical clustering investigating relative fold changes and mapping to Omicsnet protein interaction network. *CXCL10*, *CEACAM1*, *PECAM1*, *KIT*, *COL4A2*, *COL1A1*, and *HSPG2* genes were more than 50-fold up-regulated in all diagnosis groups when compared to control, whereas genes such as *ANGPT4*, *PDGFRB*, and *SERPINF1* were down-regulated only in SCLC and melanoma groups, respectively. Using hierarchical clustering, 12 out of 15 cases were allocated to the correct histological primary tumor type. We identified genes with consistent up-regulation in BM of lung cancer and melanoma and other genes with differential expression across BM of these tumor types. Our data may be of relevance for targeted therapy or prophylaxis of BM using anti-angiogenic agents.

Keywords Brain metastases · Angiogenesis · Non-small cell lung cancer · Small-cell lung cancer · Melanoma · Omicsnet

✉ Matthias Preusser
matthias.preusser@meduniwien.ac.at

[1] Department of Medicine 1, Medical University of Vienna, Vienna, Austria

[2] Department of Biomedical Engineering, University of Applied Sciences Technikum Wien, Vienna, Austria

[3] Institute for Neurology, Medical University of Vienna, Vienna, Austria

[4] Department of Neuro-Surgery, Medical University of Vienna, Vienna, Austria

[5] Department of Medicine III, Medical University of Vienna, Vienna, Austria

[6] Central Nervous System Tumour Unit, Comprehensive Cancer Center Vienna, Vienna, Austria

[7] Department of Medicine I and Comprehensive Cancer Center, Central Nervous System Tumours Unit (CCC-CNS), Medical University of Vienna, Waehringer Guertel 18-20, 1090 Vienna, Austria

Introduction

Brain metastases (BM) are the most common brain tumors of adults. The exact incidence of BM is unclear. Epidemiological studies have reported the annual incidence of BM to be approximately 11 per 100,000 persons [1]. The estimated incidence of BM among all patients with cancer is about 19 % per year. However, autopsy data show that up to 25 % of cancer patients have BM. There has been an increase of the incidence of secondary brain tumors over the past few decades, probably owing to more sensitive and widely available neuroimaging techniques, increases in survival times of cancer patients, and the increase of malignant lung neoplasms associated with smoking. The prognosis of patients with BM is poor; median survival times are typically less than 1 year.

The most common primary tumors that develop BM are lung carcinomas (35–64 %), breast carcinoma (14–18 %), melanoma (4–21 %), renal cell carcinoma, and colon carcinoma (5–10 %) [2].

The therapy of BM is limited due to the lack of prospective clinical studies [2]. Surgery and radiotherapy (stereotactic radiosurgery of isolated metastases and whole-brain radiotherapy (WBRT)) are currently the most commonly used therapeutic options in patients with BM [3–5]. Systemic treatment approaches have only little value in the multidisciplinary treatment strategy [6]. One reason is the little understanding of the brain metastatic cascade and the involved molecular mechanisms that result in the successful outgrowth of cancer cells in the brain parenchyma.

Formation of new blood vessels, angiogenesis, was proposed to be the main hallmark of cancer growth [7]. In many cancer types, angiogenesis was targeted with monoclonal antibodies or tyrosine kinase inhibitors, where an improved outcome could be observed [8, 9]. Recently, early angiogenesis was shown to be mandatory for successful macrometastasis formation in a BM mouse model [10]. This group demonstrated that chronic anti-angiogenic treatment with the anti-VEGF monoclonal antibody bevacizumab therapy prevents successful outgrowth of macrometastases of a non-squamous non-small cell lung cancer cell line to the brain. Likewise, Judah Folkman's group has found a suppressive effect of chronic anti-angiogenic therapy on micrometastatic outgrowth in the lung [11], which also supports the crucial importance of the angiogenic switch for loss of tumor dormancy in different animal models [12–14]. Interestingly, anti-angiogenic treatment was not sufficient in a brain metastasis model of melanoma [10]. Different characteristics of angiogenic and invasive growth pattern of melanoma and NSCLC brain metastases both in patients and mouse models could be demonstrated [15–18].

Based on these findings, we hypothesized that metastases to the brain from different cancer primaries might be mediated via distinct angiogenic pathways. For this purpose, genes involved in pro- and anti-angiogenic pathways were evaluated in a cohort of brain metastasis derived from different primary tumor types.

Methods

Patient population and preparation of the tissue

For this retrospective study, 15 tissue samples from patients undergoing a cerebral resection of the neuroradiologically diagnosed brain metastases were used. Six, four, and five patients had non-small cell lung cancer (NSCLC), small-cell lung cancer (SCLC), and melanoma, respectively. The surgical resections of the tumors were performed at the Department of Neurosurgery, Medical University of Vienna. Tissues were obtained during the resection and were immediately snap-frozen in OCT. The diagnosis of BM was made by the board neuropathologist after a careful review of the surgically removed tissue. This study was approved by the local ethics committee. As control, neurosurgical specimens taken from patients who underwent a surgical resection of the temporal lobe for intractable epilepsy was used.

RNA isolation

About 100 mg of frozen tissue was transferred into 1 ml of TRIzol® Reagent (Roche Diagnostics, Mannheim, Germany). Homogenization was accomplished using a Polytron power homogenization unit (Kinematica, Kriens, Switzerland). RNA was extracted by phase separation after the addition of 200 μl chloroform. The RNA-containing aqueous phase was precipitated using 500 μl isopropanol. The RNA pellet was washed twice with 75 % ethanol, briefly air-dried, redissolved in RNAse free H_2O, and either used immediately or frozen at −80 °C for later use.

Reverse transcription

After RNA extraction and purification, the reverse transcription reaction was performed. Briefly, total RNA was treated with deoxyribonuclease (DNAse) I (Invitrogen Carlsbad, CA, USA) for 15 min at room temperature, and the reaction was stopped using EDTA. The pretreated RNA was converted into complementary DNA (cDNA) using SuperScript II™ reverse transcriptase (Invitrogen Carlsbad, CA, USA) according to the manufacturer's instructions. Reaction parameters were as follows: 65 °C 15 min, 4 °C 2 min, 25 °C 4 min, 42 °C 50 min, and 65 °C 10 min. The cDNA product was diluted using DNAse-free water and either immediately used or frozen at −80 °C.

Applied biosystems gene array

The TaqMan® Array 96-well Human Angiogenesis Plate contains 92 assays for angiogenesis and lymphangiogenesis-associated genes and 4 assays for candidate endogenous control genes (Catalogue Number: 4391016, Applied Biosystems). The panel of assays in the TaqMan® Array 96-well Human Angiogenesis Plate targets known angiogenesis growth factors like *VEGF* as well as matrix-derived inhibitors such as endostatin. Additionally, the panel contains markers and targets for angiogenesis and lymphangiogenesis.

Each inventoried TaqMan® gene expression assay contains sequence-specific, unlabeled primers, and a FAM™ dye-labeled probe (Table 1). The probes are pre-coated and dried on to each well. The assays are reconstituted to a 1× formulation. Each assay plate contains four housekeeping genes (first

Table 1 Ninety-six genes involved in the gene chip which was commercially available by Applied Biosystems (ABI)

#	Assay ID	Gene symbol
1	Hs99999901_s1	*18s*
2	Hs99999905_m1	GAPDH
3	Hs99999909_m1	HPRT1
4	Hs99999908_m1	GUSB
5	Hs00241027_m1	FGA
6	Hs00264877_m1	PLG
7	Hs00166654_m1	SERPINC1
8	Hs00168730_m1	PRL
9	Hs00234422_m	MMP2
10	Hs02379000_s1	ANG
11	Hs00181613_m1	ANGPT1
12	Hs00169867_m1	ANGPT2
13	Hs00171022_m1	CXCL12
14	Hs00174781_m1	EDIL3
15	Hs00362096_m1	EPHB2
16	Hs00265254_m1	FGF1
17	Hs00266645_m1	FGF2
18	Hs00173564_m1	FGF4
19	Hs00246256_m1	FST
20	Hs00300159_m1	HGF
21	Hs00174103_m1	IL8
22	Hs00174877_m1	LEP
23	Hs00171064_m1	MDK
24	Hs00157317_m1	TYMP
25	Hs00234042_m1	PDGFB
26	Hs00383235_m1	PTN
27	Hs00260905_m1	PROK1
28	Hs00608187_m1	TGFA
29	Hs99999918_m1	TGFB1
30	Hs00174128_m1	TNF
31	Hs00900054_m1	VEGFA
32	Hs00173634_m1	VEGFB
33	Hs00153458_m1	VEGFC
34	Hs00170014_m1	CTGF
35	Hs00197064_m1	FBLN5
36	Hs00962914_m1	THBS1
37	Hs00270802_s1	TNFSF15
38	Hs00168433_m1	ITGA4
39	Hs01077958_s1	IFNB1
40	Hs00174143_vm1	IFNG
41	Hs00171042_m1	CXCL10
42	Hs00168405_vm1	IL12A
43	Hs00171467_m1	SERPINF1
44	Hs00427220_g1	PF4
45	Hs00208609_m1	VASH1
46	Hs00199608_m1	ADAMTS1
47	Hs00559786_m1	ANGPTL1
48	Hs00611096_m1	AMOT
49	Hs00153304_vm1	CD44
50	Hs00174344_m1	CDH5
51	Hs00601975_m1	CXCL2
52	Hs00184728_m1	SERPINB5
53	Hs00176573_m1	FLT1
54	Hs00188273_m1	SEMA3F
55	Hs00176096_vm1	TEK
56	Hs00178500_m1	TIE1
57	Hs00223332_m1	TNMD
58	Hs00234278_m1	TIMP2
59	Hs00165949_m1	TIMP3
60	Hs00765775_m1	ANGPTL2
61	Hs00205581_m1	ANGPTL3
62	Hs00236077_m1	CEACAM1
63	Hs00232618_m1	HEY1
64	vHs00233808_m1	ITGAV
65	Hs00169777_m1	PECAM1
66	Hs00272659_m1	LYVE1
67	Hs00174029_m1	KIT
68	Hs00913333_m1	TNNI1
69	Hs00187290_m1v	NRP2
70	Hs00176676_m1	KDR
71	Hs00196470_m1	ENPP2
72	Hs00189521_m1	FIGF
73	Hs00270951_s1	FOXC2
74	Hs00266237_m1	COL4A1
75	Hs01098873_m1	COL4A2
76	Hs00266332_m1	COL15A1
77	Hs00194179_m1	HSPG2
78	Hs00181017_m1	COL18A1
79	Hs01549940_m1	FN1
80	Hs01022527_m1	COL4A3
81	Hs01011995_g1	F2
82	Hs01105174_m1	BAI1
83	Hs00900373_m1	CHGA
84	Hs00211115_m1	ANGPT4
85	Hs99999083_m1	CSF3
86	Hs00963711_g1	GRN
87	Hs01568063_m1	THBS2
88	Hs00993254_m1	LECT1
89	Hs01101127_m1	ANGPTL4
90	Hs01001469_m1	ITGB3
91	Hs00998026_m1	PDGFRA
92	Hs00387364_m1	PDGFRB
93	Hs01047677_m1	FLT4
94	Hs00826128_m1	NRP1
95	Hs01922614_s1	S1PR1
96	Hs00896294_m1	PROX1

four genes listed in Table 1). A reaction volume of 10 μl was applied into each well. cDNA concentration was adjusted for 50 ng for each reaction well. For the whole plate, a total reaction volume of 1080 μl including 12.5 % excess volume was prepared. This included 540 μl of cDNA + DNase-free water and TaqMan® Fast Universal Master Mix (Catalogue Number: 4352042, Applied Biosystems). The plate was covered with a MicroAmp® Optical Adhesive Film and was read at the suggested thermal cycling condition of the Step One Plus™ Real Time PCR Systems, all described in the test manual (Applied Biosystems, Forster City, CA, USA).

Biostatistical evaluation of the data and in silico analyses

Data preprocessing

Raw data for the given probes consisted of cycle time (Ct values) from the Real Time PCR System. In the first step, a screening for missing Ct values was performed. Considering possible technical errors with the chip, genes having detectable Ct values in less than five samples (<33.3 %) were omitted from the analysis. For genes having Ct values in five or more samples (>=33 %), missing values are interpreted as no gene expression present and these Ct values were set to the cutoff of 45 cycles. In the second step, outliers with implausible high expression rates (mean—3* standard deviation) of a given sample were replaced by the mean Ct value of the other samples of the same group. Finally, normalization and relative fold change calculation of the gene expression compared to the control reference tissue was analyzed according to the ΔΔCt method [19].

Hierarchical clustering

Normalized data was hierarchically clustered using Pearson correlation as distance with average linkage rule utilizing the MultiExperiment Viewer software version 4.9 (Dana Farber Cancer Institute, Boston, MA, USA).

Gene expression analysis

An analysis of differences in gene expression between study groups was performed by calculating the average relative fold change for each gene for each patient group. Three cutoffs for the relative fold change were defined (50-fold, 10-fold, and 2-fold). Overlaps and differences of the relative fold change between the study groups were counted for each gene.

Network analysis

The angiogenesis chip gene set was mapped to Omicsnet protein interaction network version Feb. 2013 [20, 21]. Additionally, proteins were added to connect the angiogenesis chip set to form a spanning tree within Omicsnet utilizing a modified minimum spanning tree [22] algorithm based on Prim [23] and Kruskal [24]. Edges of experimentally verified protein-protein interactions were highlighted. Conspicuities of the

Table 2 Clinical and demographic data of the patient population

Patient ID	Gender	Age (years)	Primary tumor	CHT before BM	BMFS (months)	Metastases extracranial	BM number	OS (days)
1	w	60	NSCLC	No	0	0	3	226
2	w	57	NSCLC	No	163	1	1	812
3	m	56	NSCLC	Yes	0	2	1	22
4	w	56	NSCLC	Yes	32	0	1	91
5	w	49	NSCLC	Yes	27	0	1	209
6	m	79	NSCLC	No	0	0	1	80
7	m	64	SLCL	No	0	0	2	166
8	w	61	SLCL	No	0	5	1	896
9	m	60	SLCL	Yes	29	0	2	112
10	m	75	SLCL	No	89	0	1	27
11	m	72	Melanoma	Yes	124	0	1	40
12	w	47	Melanoma	Yes	18	2	3	608
13	w		Melanoma					287
14	w	54	Melanoma	No	0	0	1	226
15	w	32	Melanoma	Yes	185	1	2	97

Age, at the time of brain metastases

f female, *m* male, *NSCLC* non-small cell lung cancer, *SCLC* small-cell lung cancer, *CHT* chemotherapy, *BM* brain metastases, *BMFS* brain metastases free survival, *OS* overall survival after diagnosis of BM

interaction neighborhood of up- and down-regulated genes were described.

Results

Study population and demographic data

Demographic and clinical data of the patient population is depicted in Table 2. Seven (7/15, 47 %) patients received chemotherapy due to primary tumor before manifestation of BM. In six patients (6/15, 40 %), the primary tumor and BM were diagnosed at the same time. The median brain metastases free survival (BMFS) of the whole cohort was 22.5 months ranging between 27 and 185 months. Five (5/15, 34 %) patients represented metastases out of the brain. Five (5/15, 34 %) patients were diagnosed with more than one intracranial metastasis. Overall survival (OS) after diagnosis of BM was 166 days ranging between 22 and 896 days within the entire population.

Table 3 Genes, which are up/down-regulated more than 50-fold and 10-fold in all study groups and only in one of the study group but not in others

		Up-regulation	Down-regulation
50-fold	NSCLC + SCLC + melanoma	*CXCL10*	
		CEACAM1	
		PECAM1	
		KIT	
		COL4A2	
		COL15A1	
		HSPG2	
	NSCLC		
	SCLC	*ANGPT4*	*TGFB1*
		PDGFRB	
	Melanoma	*SERPINF1*	
10-fold	NSCLC + SCLC + melanoma	*TNF*	*S1PR1*
		VEGFA	*CHGA*
		FBLN5	*ENPP2*
		ITGA4	*PROX1*
		HEY1	*EDIL3*
		LYVE1	
		CDH5	
		FST	
		COL4A1	
		CD44	
	NSCLC	*SEMA3F*	*FOXC2*
		FLT1	
	SCLC	*IFNB1*	
	Melanoma	*MMP2*	*CSF3*
		ANGPT2	*VASH1*
		ADAMTS1	*PDGFRA*
		TIMP2	*EPHB3*
		NRP2	
		ITGB3	

NSCLC non-small cell lung cancer, *SCLC* small-cell lung cancer

Gene expression data and differentially regulated genes

Out of 4 housekeeping genes included in the gene chip, only *GUSB* had detectable Ct values in all patient samples. Normalization of the gene expression data was performed based on this house keeping gene. Genes having detectable expression values in less than 5 samples among 15 patients were removed from the dataset (*PLG*, *ANGPTL3*, *FGF4*, *SERPINB5*, *COL4A3*, *TNNI1*, *LECT1*, *IFNG*) leading to a reduction of the gene set size to 84 genes. Four genes represented no detectable Ct values in the control brain tissue (*TNMD*, *PRL*, *LEP*, *F2*). *ANGPTL1* in #2 and *BAI* in #13 were identified as extreme outliers and were modified accordingly.

Gene expression analysis revealed seven genes as up-regulated more than 50-fold in all study groups, whereas none of the genes was down-regulated 50-fold in the entire cohort when compared to that of control brain tissue (Table 3). Interestingly, some genes were down-regulated 50-fold only in a certain entity but not in others, like *ANGPT4 and PDGFRB* for SCLC and *SERPINF1* for melanoma. Table 3 depicts the genes, which are up/down-regulated more than 50-fold and 10-fold and the genes, which were up/down-regulated only in one of the study group but not in others.

Hierarchical clustering according to the gene expression pattern

Gene expression data has been investigated for their potential to form hierarchical clusters as described in the methods section. Hierarchical clustering revealed four groups matching partially the study group definitions (Fig. 1). The first and second group demonstrated four out of the six NSCLC samples (#1,#2,#4,#6) forming a tight group next to a group of three out of the four SCLC samples (#7,#8,#9), respectively. The third group consists of two of the five melanoma samples (#12,#14) sharing similarities with a NSCLC sample (#5). The samples of the forth group have a greater distance within than any of the former groups and consists of the remainder melanoma samples (#11,#13,#15) and a sample from NSCLC (#3). One sample from the SCLC group (#10) shares the least similarities with any of the other groups.

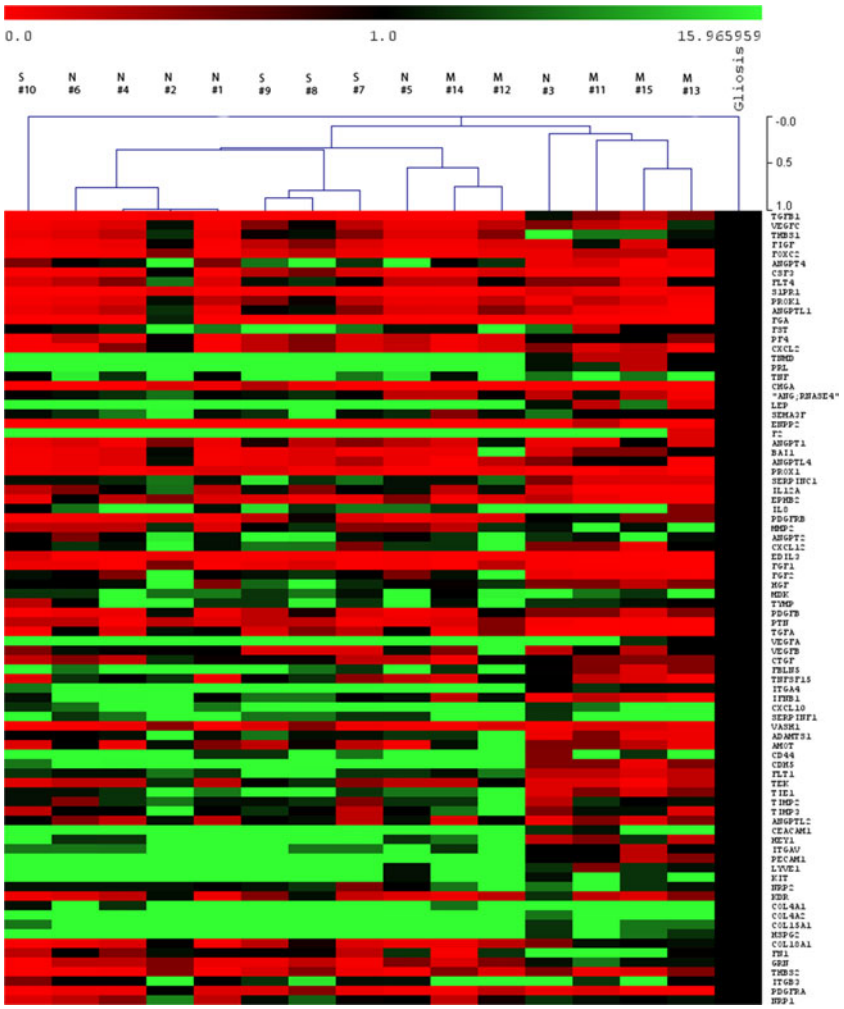

Fig. 1 Hierarchical cluster analyses based on the angiogenic relative gene expression pattern of the whole cohort. Pearson correlation as distance metric and average linkage rule. Genes are represented *above the color bars* of the image ranging from 1 to 0, indicating the degree of similarity for each patient to the next one, where they are connected with linkage bars. Patient IDs and the one control sample are indicated on the *top* of each column. Gene names are depicted on the right sight of the image. *Color bar* demonstrates the intensity of gene expression from down- to up-regulation (left to right, respectively). *S* small-cell lung cancer, *N* non-small cell lung cancer, *M* melanoma

Networking of highly differentially regulated genes

Gene sets and their fold change categories were applied to Omicsnet protein interaction network for identifying patterns of up- or down-regulation in conjunction with their protein neighborhood as well as identifying other proteins of importance in their local vicinity. The following genes from angiogenesis set were missing in Omicsnet: *ANGPTL1*, *TNMD*, *ANGPTL2*, and *PECAM1*. The following genes were added to the overview, in order to establish a connecting subgraph of the angiogenesis set: *EP300*, *MYL4*, *RPP14*, *GFI1B*, *CAPZB*, *ATXN7*, *DMP1*, *HSPA5*, *MYOC*, *MYC*, *SLC9A1*, *HDAC1*, *HSP90AA1*, and *MAGI3*. Networks for NSCLC, SCLC, and melanoma are demonstrated in Fig. 2a–c, respectively. Green proteins represent for up-regulation, whereas red proteins were the down-regulated ones. The degree of up or down-regulation correlates with the size of the green or red shapes, respectively. White symbols are the proteins with no change at the expression level, and the yellow proteins represent those, which were added for establishing a connected subgraph. From the whole set of interaction edges of Omicsnet, the interaction edges illustrated are experimentally verified.

Based on these findings, *THBS*, *MMP2*, and *FN1* could be identified as genes with the highest network capacity with more than 10 experimentally confirmed connections for each. Interestingly, for NSCLC, SCLC, and melanoma, proteins like *EP300*, *MYC*, and *HSP90AA1* linked to several up- and down-regulated angiogenic factors. As indicated above, these proteins were not a part of the angiogenesis kit but were included for connecting the angiogenesis kit set within Omicsnet.

Fig. 2 **a** Network formation based on the genes expressed in non-small cell lung cancer samples. **b** Network formation based on the genes expressed in small-cell lung cancer samples. **c** Network formation based on the genes expressed in melanoma samples. In all figures, up-regulated genes are represented in *green color*, whereas down-regulated genes are shown in *red*. The size of the genes correlated with the degree of either down- or up-regulation. *Squared shape* stays for the genes which had no expression in the control brain tissue. Genes with the *yellow color* are included to the network for establishing a connected subgraph. Genes with *white circle* had similar expression level compared to the control sample. Edges illustrated are experimentally verified

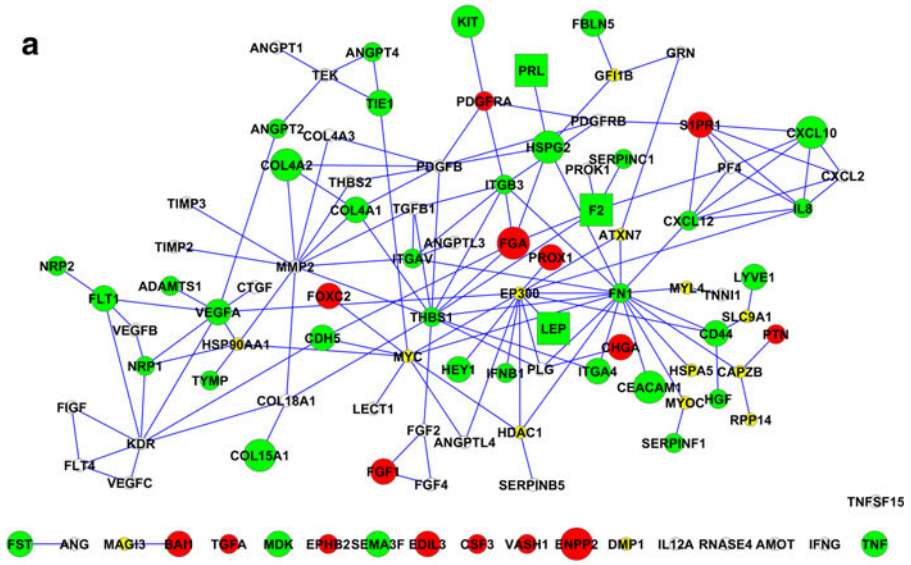
a
KIT
FBLN5
ANGPT1
ANGPT4
PRL
GRN
TEK
GFI1B
TIE1
PDGFRA
PDGFRB
S1PR1
CXCL10
ANGPT2
COL4A3
HSPG2
SERPINC1
COL4A2
PDGFB
PROK1
PF4
CXCL2
THBS2
ITGB3
TIMP3
F2
IL8
COL4A1
TGFB1
CXCL12
ATXN7
ANGPTL3
FGA
TIMP2
ITGAV
PROX1
MMP2
NRP2
LYVE1
ADAMTS1
CTGF
FOXC2
EP300
FN1
MYL4
TNNI1
FLT1
VEGFA
THBS1
SLC9A1
LEP
VEGFB
CD44
PTN
HSP90AA1
CDH5
CHGA
NRP1
MYC
HEY1
IFNB1
PLG
ITGA4
HSPA5
CAPZB
TYMP
CEACAM1
MYOC
HGF
FIGF
COL18A1
LECT1
RPP14
FGF2
HDAC1
KDR
ANGPTL4
SERPINF1
COL15A1
FLT4
FGF1
FGF4
SERPINB5
VEGFC
TNFSF15
FST
ANG
MAGI3
BAI1
TGFA
MDK
EPHB2
SEMA3F
EDIL3
CSF3
VASH1
ENPP2
DMP1
IL12A
RNASE4
AMOT
IFNG
TNF

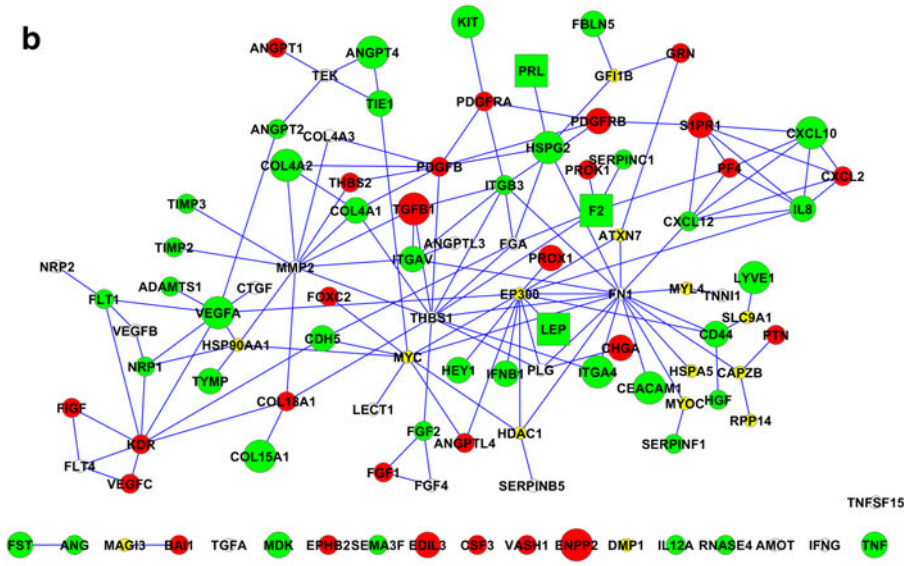
b
KIT
FBLN5
ANGPT1
ANGPT4
PRL
GRN
TEK
GFI1B
TIE1
PDGFRA
PDGFRB
S1PR1
CXCL10
ANGPT2
COL4A3
HSPG2
SERPINC1
COL4A2
PDGFB
PROK1
PF4
CXCL2
THBS2
ITGB3
TIMP3
F2
IL8
COL4A1
TGFB1
CXCL12
ATXN7
ANGPTL3
FGA
TIMP2
ITGAV
PROX1
MMP2
NRP2
LYVE1
ADAMTS1
CTGF
FOXC2
EP300
FN1
MYL4
TNNI1
FLT1
VEGFA
THBS1
SLC9A1
LEP
VEGFB
CD44
PTN
HSP90AA1
CDH5
CHGA
NRP1
MYC
HEY1
IFNB1
PLG
ITGA4
HSPA5
CAPZB
TYMP
CEACAM1
MYOC
HGF
FIGF
COL18A1
LECT1
RPP14
FGF2
HDAC1
KDR
ANGPTL4
SERPINF1
COL15A1
FLT4
FGF1
FGF4
SERPINB5
VEGFC
TNFSF15
FST
ANG
MAGI3
BAI1
TGFA
MDK
EPHB2
SEMA3F
EDIL3
CSF3
VASH1
ENPP2
DMP1
IL12A
RNASE4
AMOT
IFNG
TNF

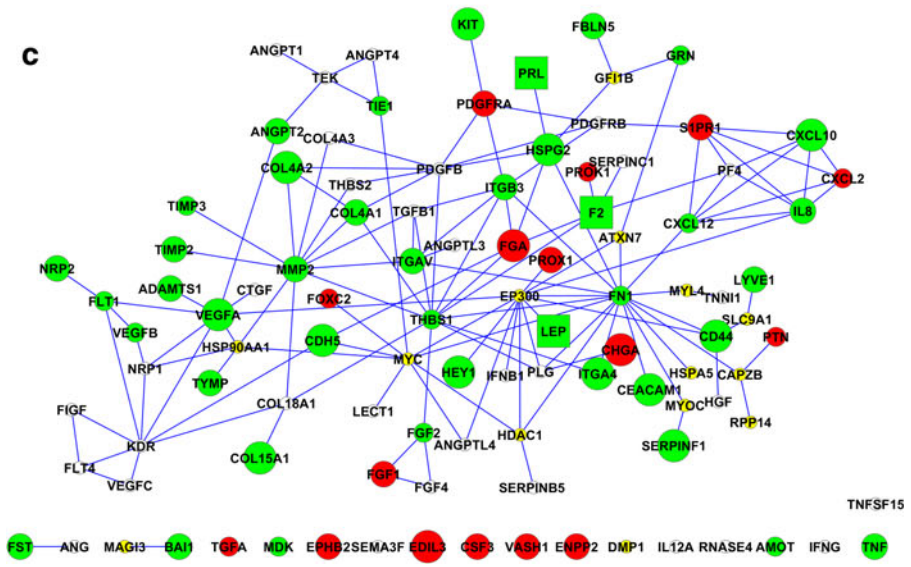
c
KIT
FBLN5
ANGPT1
ANGPT4
PRL
GRN
TEK
GFI1B
TIE1
PDGFRA
PDGFRB
S1PR1
CXCL10
ANGPT2
COL4A3
HSPG2
SERPINC1
COL4A2
PDGFB
PROK1
PF4
CXCL2
THBS2
ITGB3
TIMP3
F2
IL8
COL4A1
TGFB1
CXCL12
ATXN7
ANGPTL3
FGA
TIMP2
ITGAV
PROX1
MMP2
NRP2
LYVE1
ADAMTS1
CTGF
FOXC2
EP300
FN1
MYL4
TNNI1
FLT1
VEGFA
THBS1
SLC9A1
LEP
VEGFB
CD44
PTN
HSP90AA1
CDH5
CHGA
NRP1
MYC
HEY1
IFNB1
PLG
ITGA4
HSPA5
CAPZB
TYMP
CEACAM1
MYOC
HGF
FIGF
COL18A1
LECT1
RPP14
FGF2
HDAC1
KDR
ANGPTL4
SERPINF1
COL15A1
FLT4
FGF1
FGF4
SERPINB5
VEGFC
TNFSF15
FST
ANG
MAGI3
BAI1
TGFA
MDK
EPHB2
SEMA3F
EDIL3
CSF3
VASH1
ENPP2
DMP1
IL12A
RNASE4
AMOT
IFNG
TNF

Discussion

In this study, we demonstrate differential expression of genes involved in angiogenesis in a cohort of brain metastasis tissue originating from three distinct primaries, namely non-small cell lung cancer, small-cell lung cancer, and melanoma. Although there seemed to exist a common angiogenic gene expression pattern in all three primaries, several genes with an exclusive expression in specific diagnostic categories were found, which was responsible for the formation of clusters of cases originating from the same primary tumor group. This suggests a characteristic angiogenic gene signature of NSCLC, SCLC, and melanoma tissues when metastasized in the brain.

Angiogenesis is a hallmark of the pathobiology of primary and secondary brain tumors, which renders anti-angiogenic treatment for these diseases very attractive [1, 25]. Attempts for treatment of brain tumor patients with anti-angiogenic substances resulted in very heterogeneous outcomes of these patients [26–28]. Particularly for BM, a different kind of angiogenesis was proposed in animal models and could also be shown in the tissue derived from humans [10, 15]. Lung cancer tissue was demonstrated to establish vascular angiogenic pattern, whereas melanomas showed a cooptive growth [10, 29]. Differences at the morphology of BM from different primaries might be responsible for this variance. In line with the previous observation of mouse models showing a clear difference of angiogenesis morphology in BM of different primaries, our data could classify patients with identical diagnosis in similar clusters based on their angiogenic gene expression signature. Genes with known involvement in angiogenic processes including *VEGFA* [7], *CEACAM1* [30], *PECAM1* [31], *CXCL12* (also known as *SDF1-α*) [32], *KIT* [33], *TNF* [34], and collagens [35, 36] were at least 10 times up-regulated in all groups indicating the necessity of those factors for the establishment of the basic characteristics of the angiogenesis process. These genes are mainly involved in proliferation of endothelial cells and activation of growth factors [30, 31, 33]. Based on the potential importance of those molecules and high representation in all tissues, a treatment strategy of BM irrespective of the primary diagnosis might rely on the inhibitory strategy of these genes.

Interestingly, some other genes exhibited a differential regulation with a restriction to a certain group. In NSCLC, *SEMA3F* and *FLT1* were up-regulated, whereas *FOXC2* was down-regulated. SEMA3F was identified to represent an anti-angiogenic molecule with inhibitory capacity of VEGF [37], whereas FLT1 is the receptor of VEGF [38], suggesting the auto-activation of anti-angiogenic mechanisms for this tumor type. Interestingly, FOXC2 plays a role in epithelial to mesenchymal transition [39], which was demonstrated to be one of the leading processes for early distant metastasis for NSCLC [40]. This underlines the importance of establishment of inhibition strategies for metastasis formation in this very common primary. In SCLC, *PDGFRB* and *ANGPTL4*, which are known for the involvement in vascular development and angiogenesis, are highly up-regulated [41], whereas *TGFB1*, a multifunctional peptide for cell proliferation, differentiation, and apoptosis, was down-regulated [42]. Interestingly, similar to NSLCL, melanomas showed an activation of some anti-angiogenic factors including *ANGPT2* [43] and *SERPINF1* (also known as pigment epithelium-derived factor (*PEDF*)) [44]. However, further molecules playing important roles in matrix degradation like *MMP2* [45], *TIMP2* [45], and *ADAMTS1* [46] were also up-regulated in the melanoma group when compared to NSCLC and SCLC. Since degradation of extracellular matrix has been highlighted in melanomas for successful metastasis, the finding of up-regulation of matrix degradation factors in melanoma BM tissues is not surprising [47]. Those particular genes might be responsible for the differences seen at the morphology of the angiogenesis in melanoma and NSCLC patients. Moreover, inhibition of matrix degradation could be considered as a mechanism, which might be primarily targeted for the treatment of melanoma BM.

Since patients with BM have been largely excluded from clinical trials with anti-angiogenic agents, we do not know whether responses to the anti-angiogenic treatments would vary between BM patients of different primary tumor. Our data and the data from others would together shed light on the potential diversity of angiogenesis of BM at the molecular basis, which might be considered for future treatment strategies and clinical trial designs as an important point for the patient selection. In future clinical trials, anti-angiogenic agents might be stratified on BM patients depending on their primary tumor. Targeting factors with a commonly high expression in all BMs (e.g., *VEGF*, *PECAM1*) might reveal a balanced outcome, whereas a strict selection of the patients based on their primary tumor might be necessary, if factors with differential expression are chosen (e.g., *SERPINF1*, *TIMP2*, and *MMT2*).

The data revealed by the gene chip was analyzed with Omicsnet in order to find out the relationships and network vicinity between differentially regulated genes. Notably, 14 genes were included to the networking schema establishing a network connection by the angiogenesis genes with several of these genes being highly connected to up- or down-regulated genes. These additional genes might also be related to the varying formation of angiogenesis in different BM primary diagnoses and should be investigated into more detail in future preclinical studies.

In this small pilot study, some limitations should be mentioned: As obtaining healthy brain tissue was not feasible, we used temporal lobe tissue from anti-epileptic surgery as control sample and compared the gene expression levels of each tumor tissue with that as control. As this approach was usual

in the literature, we hope that the gene expression level of a noncancerous tissue, namely temporal lobe, would reflect the expression level of control tissue [48]. Within the kit, which was provided commercially, four endogenous controls were available. Among those, only one endogenous control was detectable in all tissues, *GUSB*, which was used for further analyses. The lack of reliable detectability of the other three control genes remains unexplained and may relate to technical issues or inconsistent expression in the CNS. In any case, it does not influence the results of our study, as these genes were excluded from all analyses.

To sum up, we demonstrate that BM belonging to different primaries could be distinguished based on their angiogenic character. Those differences might influence the outcome of patients when treated with distinct anti-angiogenic drugs. This could be linked with the treatment armamentarium of BM patients and might be a basis for the patient selection in future clinical trials.

Conflicts of interest None

References

1. Preusser M, Capper D, Ilhan-Mutlu A, Berghoff AS, Birner P, Bartsch R, et al. Brain metastases: pathobiology and emerging targeted therapies. Acta Neuropathol. 2012;123:205–22.
2. Kienast Y, Winkler F. Therapy and prophylaxis of brain metastases. Expert Rev Anticancer Ther. 2010;10:1763–77.
3. Gaspar LE, Mehta MP, Patchell RA, Burri SH, Robinson PD, Morris RE, et al. The role of whole brain radiation therapy in the management of newly diagnosed brain metastases: a systematic review and evidence-based clinical practice guideline. J Neuro-oncol. 2010;96:17–32.
4. Kalkanis SN, Kondziolka D, Gaspar LE, Burri SH, Asher AL, Cobbs CS, et al. The role of surgical resection in the management of newly diagnosed brain metastases: a systematic review and evidence-based clinical practice guideline. J Neuro-oncol. 2010;96:33–43.
5. Linskey ME, Andrews DW, Asher AL, Burri SH, Kondziolka D, Robinson PD, et al. The role of stereotactic radiosurgery in the management of patients with newly diagnosed brain metastases: a systematic review and evidence-based clinical practice guideline. J Neuro-oncol. 2010;96:45–68.
6. Mehta MP, Paleologos NA, Mikkelsen T, Robinson PD, Ammirati M, Andrews DW, et al. The role of chemotherapy in the management of newly diagnosed brain metastases: a systematic review and evidence-based clinical practice guideline. J Neuro-oncol. 2009;96:71–83.
7. Folkman J. Angiogenesis: an organizing principle for drug discovery? Nat Rev Drug Discov. 2007;6:273–86.
8. Massard C, Zonierek J, Gross-Goupil M, Fizazi K, Szczylik C, Escudier B. Incidence of brain metastases in renal cell carcinoma treated with sorafenib. Ann Oncol. 2010;21:1027–31.
9. Soria JC, Mauguen A, Reck M, Sandler AB, Saijo N, Johnson DH, et al. Systematic review and meta-analysis of randomised, phase ii/iii trials adding bevacizumab to platinum-based chemotherapy as first-line treatment in patients with advanced non-small-cell lung cancer. Ann Oncol. 2013;24:20–30.
10. Kienast Y, von Baumgarten L, Fuhrmann M, Klinkert WE, Goldbrunner R, Herms J, et al. Real-time imaging reveals the single steps of brain metastasis formation. Nat Med. 2010;16:116–22.
11. Holmgren L, O'Reilly MS, Folkman J. Dormancy of micrometastases: balanced proliferation and apoptosis in the presence of angiogenesis suppression. Nat Med. 1995;1:149–53.
12. Indraccolo S, Stievano L, Minuzzo S, Tosello V, Esposito G, Piovan E, et al. Interruption of tumor dormancy by a transient angiogenic burst within the tumor microenvironment. Proc Natl Acad Sci U S A. 2006;103:4216–21.
13. Naumov GN, Bender E, Zurakowski D, Kang SY, Sampson D, Flynn E, et al. A model of human tumor dormancy: an angiogenic switch from the nonangiogenic phenotype. J Natl Cancer Inst. 2006;98:316–25.
14. Udagawa T, Fernandez A, Achilles EG, Folkman J, D'Amato RJ. Persistence of microscopic human cancers in mice: alterations in the angiogenic balance accompanies loss of tumor dormancy. FASEB J. 2002;16:1361–70.
15. Berghoff AS, Ilhan-Mutlu A, Dinhof C, Magerle M, Hackl M, Widhalm G, et al. Differential role of angiogenesis and tumor cell proliferation in brain metastases according to primary tumor type: analysis of 639 cases. Neuropathol Appl Neurobiol. 2014
16. Berghoff AS, Rajky O, Winkler F, Bartsch R, Furtner J, Hainfellner JA, et al. Invasion patterns in brain metastases of solid cancers. Neuro-Oncology. 2013;15:1664–72.
17. Berghoff AS, Bartsch R, Wohrer A, Streubel B, Birner P, Kros JM, et al. Predictive molecular markers in metastases to the central nervous system: recent advances and future avenues. Acta Neuropathol. 2014
18. Berghoff AS, Ilhan-Mutlu A, Wohrer A, Hackl M, Widhalm G, Hainfellner JA, et al. Prognostic significance of ki67 proliferation index, hif1 alpha index and microvascular density in patients with non-small cell lung cancer brain metastases. Strahlenther Onkol. 2014;190:676–85.
19. Livak KJ, Schmittgen TD. Analysis of relative gene expression data using real-time quantitative pcr and the 2(−delta delta c(t)) method. Methods. 2001;25:402–8.
20. Bernthaler A, Muhlberger I, Fechete R, Perco P, Lukas A, Mayer B. A dependency graph approach for the analysis of differential gene expression profiles. Mol BioSyst. 2009;5:1720–31.
21. Fechete RHA, Söllner J, Perco P, Lukas A, Mayer B. Using information content for expanding human protein coding gene interaction networks. J Comp Sci Syst Biol. 2013;6:073–82.
22. Siehs C. Simulation in metabolic networks. TU Vienna: Faculty of Bioinformatics; 2015.
23. Prim RC. Shortest connection networks and some generalisations. Bell Syst Tech J. 1957;36:1389–401.
24. Kruskal J. On the shortest spanning subtree and the traveling salesman problem. Proc Am Math Soc. 1956;7:48–50.
25. Preusser M, Berghoff AS, Schadendorf D, Lin NU, Stupp R. Brain metastasis: opportunity for drug development? Curr Opin Neurol. 2012;25:786–94.
26. Gilbert MR, Dignam JJ, Armstrong TS, Wefel JS, Blumenthal DT, Vogelbaum MA, et al. A randomized trial of bevacizumab for newly diagnosed glioblastoma. N Engl J Med. 2014;370:699–708.
27. Chinot OL, Wick W, Mason W, Henriksson R, Saran F, Nishikawa R, et al. Bevacizumab plus radiotherapy-temozolomide for newly diagnosed glioblastoma. N Engl J Med. 2014;370:709–22.
28. Kreisl TN, Kim L, Moore K, Duic P, Royce C, Stroud I, et al. Phase ii trial of single-agent bevacizumab followed by bevacizumab plus irinotecan at tumor progression in recurrent glioblastoma. J Clin Oncol. 2009;27:740–5.
29. Leenders WP, Kusters B, Verrijp K, Maass C, Wesseling P, Heerschap A, et al. Antiangiogenic therapy of cerebral melanoma metastases results in sustained tumor progression via vessel co-option. Clin Cancer Res. 2004;10:6222–30.

30. Gerstel D, Wegwitz F, Jannasch K, Ludewig P, Scheike K, Alves F, et al. Ceacam1 creates a pro-angiogenic tumor microenvironment that supports tumor vessel maturation. Oncogene. 2011;30:4275–88.
31. Cao G, O'Brien CD, Zhou Z, Sanders SM, Greenbaum JN, Makrigiannakis A, et al. Involvement of human pecam-1 in angiogenesis and in vitro endothelial cell migration. Am J Physiol Cell Physiol. 2002;282:C1181–90.
32. Zheng H, Fu G, Dai T, Huang H. Migration of endothelial progenitor cells mediated by stromal cell-derived factor-1alpha/cxcr4 via pi3k/akt/enos signal transduction pathway. J Cardiovasc Pharmacol. 2007;50:274–80.
33. Yarden Y, Kuang WJ, Yang-Feng T, Coussens L, Munemitsu S, Dull TJ, et al. Human proto-oncogene c-kit: a new cell surface receptor tyrosine kinase for an unidentified ligand. EMBO J. 1987;6:3341–51.
34. Pan S, An P, Zhang R, He X, Yin G, Min W. Etk/bmx as a tumor necrosis factor receptor type 2-specific kinase: role in endothelial cell migration and angiogenesis. Mol Cell Biol. 2002;22:7512–23.
35. Hwang-Bo J, Yoo KH, Park JH, Jeong HS, Chung IS. Recombinant canstatin inhibits angiopoietin-1-induced angiogenesis and lymphangiogenesis. Int J Cancer. 2012;131:298–309.
36. Harris A, Harris H, Hollingsworth MA. Complete suppression of tumor formation by high levels of basement membrane collagen. Mol Cancer Res. 2007;5:1241–5.
37. Gaur P, Bielenberg DR, Samuel S, Bose D, Zhou Y, Gray MJ, et al. Role of class 3 semaphorins and their receptors in tumor growth and angiogenesis. Clin Cancer Res. 2009;15:6763–70.
38. Chappell JC, Mouillesseaux KP, Bautch VL. Flt-1 (vascular endothelial growth factor receptor-1) is essential for the vascular endothelial growth factor-notch feedback loop during angiogenesis. Arterioscler Thromb Vasc Biol. 2013;33:1952–9.
39. Sipos F, Galamb O. Epithelial-to-mesenchymal and mesenchymal-to-epithelial transitions in the colon. World J Gastroenterol. 2012;18:601–8.
40. Denlinger CE, Ikonomidis JS, Reed CE, Spinale FG. Epithelial to mesenchymal transition: the doorway to metastasis in human lung cancers. J Thorac Cardiovasc Surg. 2010;140:505–13.
41. Lee HJ, Cho CH, Hwang SJ, Choi HH, Kim KT, Ahn SY, et al. Biological characterization of angiopoietin-3 and angiopoietin-4. FASEB J. 2004;18:1200–8.
42. Prud'homme GJ. Pathobiology of transforming growth factor beta in cancer, fibrosis and immunologic disease, and therapeutic considerations. Lab Investig. 2007;87:1077–91.
43. Maisonpierre PC, Suri C, Jones PF, Bartunkova S, Wiegand SJ, Radziejewski C, et al. Angiopoietin-2, a natural antagonist for tie2 that disrupts in vivo angiogenesis. Science. 1997;277:55–60.
44. Alcantara MB, Nemazannikova N, Elahy M, Dass CR. Pigment epithelium-derived factor upregulates collagen i and downregulates matrix metalloproteinase 2 in osteosarcoma cells, and colocalises to collagen i and heat shock protein 47 in fetal and adult bone. J Pharm Pharmacol. 2014;66:1586–92.
45. Sounni NE, Janssen M, Foidart JM, Noel A. Membrane type-1 matrix metalloproteinase and timp-2 in tumor angiogenesis. Matrix Biol. 2003;22:55–61.
46. Kuno K, Kanada N, Nakashima E, Fujiki F, Ichimura F, Matsushima K. Molecular cloning of a gene encoding a new type of metalloproteinase-disintegrin family protein with thrombospondin motifs as an inflammation associated gene. J Biol Chem. 1997;272:556–62.
47. Orgaz JL, Sanz-Moreno V. Emerging molecular targets in melanoma invasion and metastasis. Pigment Cell Melanoma Res. 2013;26:39–57.
48. Ilhan-Mutlu A, Wohrer A, Berghoff AS, Widhalm G, Marosi C, Wagner L, et al. Comparison of microrna expression levels between initial and recurrent glioblastoma specimens. J Neuro-oncol. 2013;112:347–54.